**West-East High Speed Flow Field Conference**
**19-22, November 2007**
**Moscow, Russia**

# SHOCK WAVES AT MICROSCALESN

**D. E. Zeitoun[1] Y. Burtschell[1] I.A. Graur[1] M. S. Ivanov[2]**
**A. N. Kudryavtsev[2] Ye. A. Bondar[2]**

[1] *Université de Provence, Ecole Polytechnique Universitaire de Marseille–DME, 13453 Marseiile (France)*
[2] *ITAM, Siberian Division of Russian Academy of Sciences, 630090 Novosibirsk (Russia)*

**Key words:** Shock wave propagation, rarefaction effects, different flow scales

**Abstract.** Numerical simulation of shock wave propagation in microchannels and microtubes has been performed using three different approaches: the Navier-Stokes equations with the velocity slip and temperature jump boundary conditions, the statistical Direct Simulation Monte Carlo (DSMC) method for the Boltzmann equation, and the model kinetic Bhatnagar-Gross-Krook (BGK) equation. The influence of the viscosity and heat-conductivity, the wall heat transfer losses, and the rarefaction effects has been studied and the results obtained with different approaches have been compared.

## 1. INTRODUCTION

A rapid progress in micromachining techniques during the last two decades has resulted in the fabrication and utilization of micro-electromechanical systems (MEMS) and nano-electromechanical systems (NEMS). In the aerospace applications, many micromachines, such as micropumps, microturbines, microvalves, micronozzles etc. involve flows of gases (or liquids), both in subsonic and supersonic speed range. Due to very small size of MEMS, flows in them have many important features that are different from those in macromachines. An important problem in the development of MEMS is the design of devices that are able to produce mechanical work from chemical heat release, i.e. the micro-engines. At the miniaturization level, the time scales associated with heat loss mechanisms are reduced dramatically while the characteristic time scales for heat release stay virtually independent of scale. Thus, the efficiency of conventional devices such as internal combustion engines and gas turbines is seriously degraded when they are scaled to small sizes. One possibility to overcome this difficulty is to increase the rapidity of heat release using shock-induced (and/or shock-assisted) combustion. However, this technique requires a deeper insight into the mechanisms governing the microscale shock wave phenomena. The effects of viscosity and heat-conductivity, the heat losses due to the wall heat transfer, the non-equilibrium phenomena observed in rarefied flows are of importance for shock wave propagation and interaction at microscales while they are usually can be neglected for macroscale shock waves.

The investigations of viscous and rarefaction effects on shock wave propagation in shock tubes at low initial pressure were started many years ago.[1–3] The most prominent phenomena observed and investigated in these studies were shock wave deceleration, contact surface acceleration and, as a result, a significant decrease in time interval between the arrivals of the shock wave and the contact surface. Recently, a renewed interest to shock waves at microscales resulted in new experimental and numerical studies of these phenomena.[4–6]

Numerical investigations of gas microflows require the development of appropriate and efficient numerical tools. If the flow Knudsen number $\mathrm{Kn} = \ell/L < 0.1$ (where $\ell$ is the mean free molecular path and $L$ is characteristic length scale) then the continuum description based on the Navier-Stokes equations with the wall boundary conditions, which take into account the velocity slip and temperature jump, can be generally applied. Otherwise, the kinetic approach based on the Boltzmann equation for the distribution function should be invoked. The most well-known numerical tool for solving the Boltzmann equation is the Direct Simulation Monte Carlo (DSMC) method, which, in recent decades, was successfully used for the simulation of various rarefied flows, especially in the aerospace applications. However, like any statistical techniques, the DSMC method suffers from the statistical noise, this problem is particularly severe for low-speed and/or unsteady microflows. Another approach, which one considers as a promising alternative, is the direct solution of kinetic equations with high-resolution finite-difference schemes. Since the direct finite-difference solution of the Boltzmann equation is very resource-consuming due to the complicated form of its collision integral term, the model kinetic equation, such as the Bhatnagar-Gross-Krook (BGK) one, can be solved instead. In the model equation the collision integral is replaced by a simple term describing relaxation to the equilibrium distribution function.

The primary objective of the present paper is to simulate numerically the shock wave propagation in the microscale channels and tubes using all three above-mentioned techniques. The investigation is aimed at both validating the numerical solvers for their applications to microflows and better elucidating the physical phenomena accompanying the shock waves at microscales.

## 2. NUMERICAL TECHNIQUES

The unsteady flow in a micro shock tube (plane microchannel or round microtube) which occurs after the rupture of a diaphragm separating initially the gases at different pressures is considered solving the Navier-Stokes, Boltzmann and BGK equations.

Two different compressible Navier-Stokes codes are used for continuum modeling of the viscosity and heat-conductivity effects on shock wave propagation at microscales: the CARBUR solver developed at IUSTI[7] and the solver from ITAM.[8] Both the codes solve the Navier-Stokes equations on a structured quadrilateral grid using modern high-resolution shock-capturing schemes for evaluating the convective fluxes and the central finite differences to calculate the diffusive terms. An additional feature of the CARBUR code is its capability of simulating multispecies and chemically reacting flows.

Rarefaction effects are taken into account by imposing the velocity slip and temperature jump boundary conditions on the solid wall deduced from from an approx-

imate solution of the kinetic equation in the Knudsen layer.[9]

The DSMC computations were performed using the SMILE software system[10] developed at the ITAM and based on the majorant frequency scheme. SMILE employs two independent grids: the first one to organize particle collisions, and the second one for sampling of macroparameters. Both grids are based on uniform rectangular background cells, which are split into smaller cells, if necessary. The collisions between the molecules are performed using the Variable Hard Sphere (VHS) model, the diffuse reflection model with complete energy accommodation is employed at the channel wall.

The BGK-type model kinetic equation for the distribution function $f(\mathbf{x}, \mathbf{v}, t)$

$$\frac{\partial f}{\partial t} + \mathbf{v} \cdot \frac{\partial f}{\partial \mathbf{x}} = \nu \left( f^{eq} - f \right), \tag{1}$$

where $f^{eq}$ is the equilibrium distribution function, $\mathbf{v}$ is the molecular velocity, $\nu = p/\mu$ is the collision frequency ($p$ is the pressure) has been solved with a finite-difference solver based on the discrete ordinate method in the velocity space and the 3rd or 5th order WENO scheme[11] in the coordinate space. The numerical integration in the velocity space is performed using the composite Simpson rule. The Maxwell diffuse reflection boundary condition is imposed on the distribution function at the wall surface.

It is well known that the original BGK equation with the Maxwellian equilibrium distribution function leads to an incorrect value of the Prandtl number. To circumvent this problem, $f^{eq}$ is modified as proposed by Shakhov[12] (S-model).

## 3. COMPARISON OF RESULTS FROM CONTINUUM AND KINETIC MODELS

All above-mentioned approaches have been applied on the same test case. The chosen test case is the propagation of a shock wave in a plane microchannel with the height $2H = 5$ mm and the length $L = 32H$. Argon is employed as both driven and driver gas. The initial pressures on two sides of the diaphragm are $p_1 = 44.2$ Pa and $p_2 = 11.9p_1$, which corresponds, in the ideal inviscid case, to Mach number $M_s^{theor} = 1.6$. The initial gas temperature is 300 K and the same value is taken for the wall temperature. At these conditions, the Knudsen numbers calculated for low-pressure and high-pressure gases are $\mathrm{Kn}_1 = \ell_1/H = 0.05$ and $\mathrm{Kn}_2 = \ell_2/H = 4.2 \cdot 10^{-3}$ respectively. The viscosity is taken proportional to $T^{0.81}$.

Owing to the problem symmetry, all computations are performed in the half of the complete domain. The Navier-Stokes simulation has been performed on the grid of 1280×40 cells. For the DSMC computations about 110 million of model particles, 1.5 million of collisional cells, and 15.000 of macroparameter cells have been used. The size of collisional cell and time step value were significantly smaller than local mean free path and local mean collision time, respectively. All presented DSMC results are obtained using time averaging over the interval of 100 time steps (=1 $\mu$s) to reduce the statistical scatter. The coordinate grid size for the BGK computations is the same as for the Navier-Stokes simulations while 33×33 points are utilized in the velocity space.

The temperature flowfields at $t = 80$ $\mu$s obtained with three different approaches are given in Fig. 1. It is evident that generally the flowfields are in good agreement,

however the DSMC results suffer from a statistical noise in the low-pressure gas. The distributions of longitudinal velocity along the line of symmetry at $t = 80$ $\mu$s

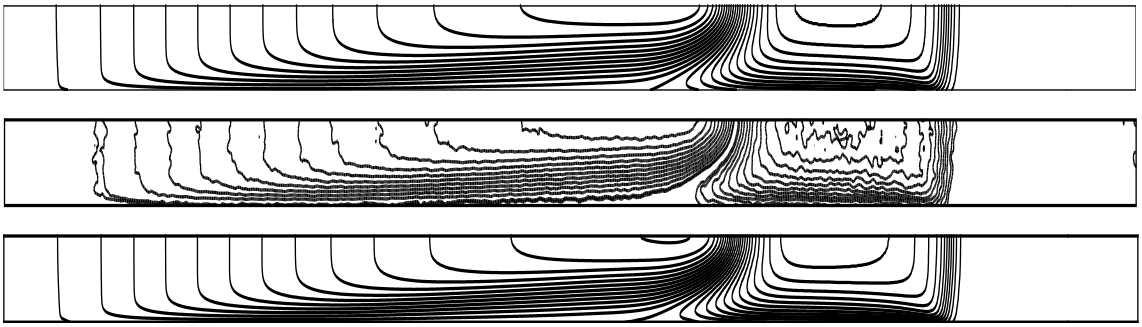

Figure 1: Temperature flowfields at $\mathrm{Kn}_1 = 0.05$ obtained in Navier-Stokes (top), DSMC (middle) and BGK (bottom) simulations.

are shown in Fig. 2.

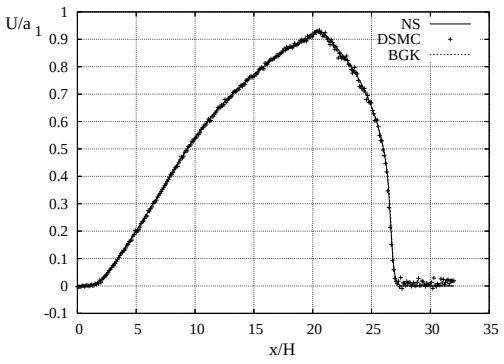


Figure 2: Velocity distributions along the line of symmetry at $\mathrm{Kn}_1 = 0.05$.

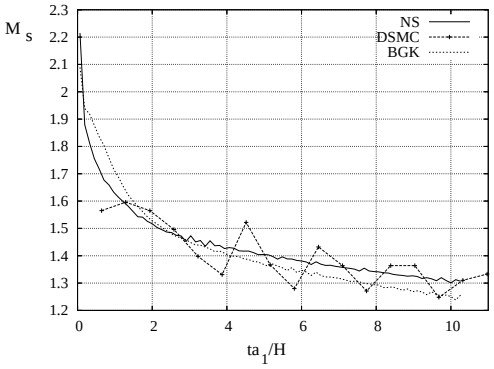


Figure 3: Shock Mach number vs time at $\mathrm{Kn}_1 = 0.05$.

The shock wave position $X_s$ and velocity have been extracted from the density distributions along the symmetry line. The time dependencies of $X_s$ in three computations are very close to one another. The shock wave Mach numbers $M_s$ as functions of non-dimensional time $\tau = ta_1/H$ (where $a_1$ is the velocity of sound in the lower-pressure gas) are given in Fig. 3. Data scattering in $M_s$ is basically due to difficulties of accurate extraction of this quantity from numerical data. At the first moments, the shock velocity exceeds the theoretical inviscid value because of viscous widening of the discontinuous initial profile. However, it rapidly decreases down to $M_s \approx 1.3$.

Numerical simulations have also been performed for tenfold decreased level of the initial pressures so that $\mathrm{Kn}_1 = 0.5$ and $\mathrm{Kn}_2 = 4.2{\cdot}10^{-2}$. The velocity distributions for this case are given in Fig. 4. As can be seen, now there is a bigger difference between the Navier-Stokes computation and two kinetic approaches. The time dependencies of $M_s$ are shown in Fig. 5. The velocities decrease rapidly and become sonic in the end of computation.

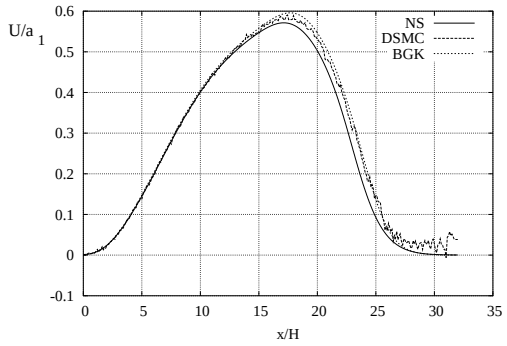


Figure 4: Velocity distributions along the line of symmetry at $\mathrm{Kn}_1 = 0.5$.

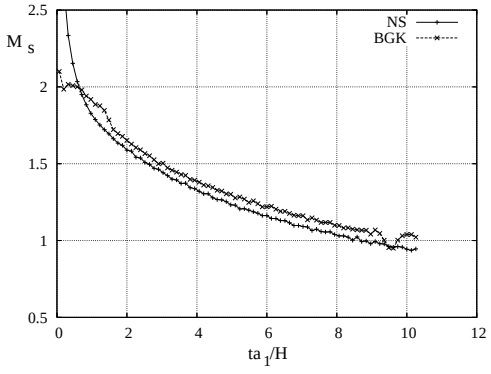


Figure 5: Shock Mach number vs time at $\mathrm{Kn}_1 = 0.5$.

## 3. PARAMETRIC STUDY OF SHOCK WAVE PROPAGATION WITH NAVIER-STOCKES SOLVER

The dependence of shock wave propagation on the Knudsen number and on the initial pressure ratio has been studied by the continuum approach. The Navier-Stokes equations have been solved for a plane microchannel with $L/H = 100$ using the grid consisting of 4000×40 cells. Three different values of $\mathrm{Kn}_1 = 0.01$, 0.05, and 0.25 have been considered at the initial pressure which correspond the theoretical shock wave Mach number $\mathrm{M}_s^{theor} = 1.6$. The obtained evolution of shock wave Mach numbers is shown in Fig. 6

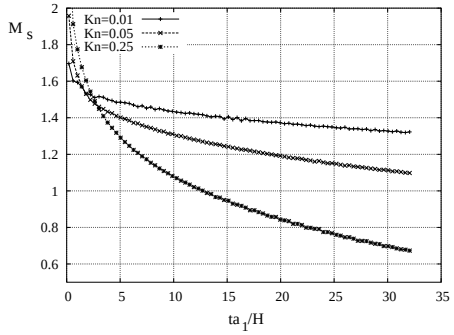


Figure 6: Shock wave Mach number at $M_s^{theor} = 1.6$ and different Knudsen numbers.

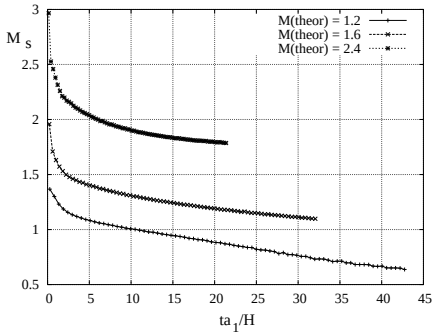


Figure 7: Shock wave Mach number at $\mathrm{Kn}_1 = 0.05$ and different $M_s^{theor}$

For the lowest value of Kn the shock wave may be hardly identified, which is probably explains the values of $\mathrm{M_s} < 1$ observed at later time moments (the shock wave position has been determined as a point where the density $\rho = 1.05\rho_1$).

Computations with the fixed $\mathrm{Kn}_1 = 0.05$ and pressure ratios corresponding to ideal Mach numbers $M_s = 1.2$, 1.6, and 2.4 have also been performed. The results are shown in Fig. 7.

## 4. SHOCK WAVE PROPAGATION FOR DIFFERENT DRIVEN AND DRIVER GASES

In order to obtain higher Mach number in microtubes, different driver/driven gases have to use. The CARBUR code[7] allows to perform these computations. A detailed numerical description of the flow in a microtube can be found in.[6] In the present study, $H_2/N_2$ are the driver/driven gases at the temperature T=300K. The diameter and the length of the tube are respectively 5 mm and 0.5 m, the pressure ratio $P_4/P_1 = 156$, which corresponds to an ideal Mach number equal to 5. The scaling ratio $S_c$=$Re_1 D/4L$, based on the low pressure tube length, is respectively equal to 0.1 for $P_1$=40 Pa and 0.025 for $P_1$=10 Pa. Figure 8 shows the shock position against time (left) and the evolution of the Mach number along the tube (right) for the two different initial low pressure. It can be noted the strong decrease of the shock strength along the tube an this effect is more and more important when the initial pressure decreases for the same pressure ratio. After only a distance of 10 cm after the diaphragm location, the shock Mach number is of 1.5 when the pressure $P_1$=10 Pa. As noted in,[6] these effects cannot describe by the previous 1D models.[3,5]

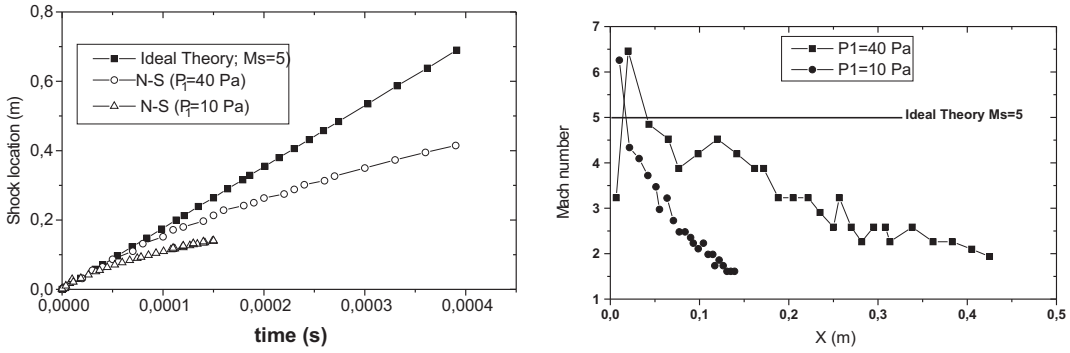


Figure 8: Shock position vs time (left) and Mach number along the tube (right).

## CONCLUSION

The shock wave propagation in the microtubes and microchannels has been studied using three different approaches. The results obtained with all three approaches are in good agreement for the investigated range of Knudsen numbers. The strong decreasing of the shock strength and its propagation velocity along the tube has been observed.

**Acknowledgments.** The authors gratefully acknowledge the support for this work from the National Center of Scientific Research (CNRS, France), project PICS-2006 and from Russian Foundation for Basic Research, RFBR project 06-01-22000.

## References

[1] Duff R. E., Shock-tube performance at low initial pressure. Phys. Fluids, vol. 2, no. 2, 1959

[2] Roshko A., On flow duration in low pressure shock tube. Phys. Fluids, vol. 3, no. 9, 1960

[3] Mirels H., Test time in low pressure shock tube. Phys. Fluids, vol. 6, no. 9, 1963

[4] Sun M., Ogawa T., Takayama K., Shock propagation in narrow channel. 23rd Int. Symposium on Shock Waves (July 22-27, 2002, Fort Worth, Texas, USA).

[5] Brouillette M., Shock waves at microscales. Shock Waves, vol. 13, no. 1, 2004

[6] Zeitoun D. E., Burtschell Y., Navier-Stokes computations in micro shock tubes. Shock Waves, vol. 15, no. 3-4, 2006

[7] Burtchell Y., Cardoso M., Zeitoun D.E. Numerical analysis of reducing driver gas contamination in impulse shock tunnels. AIAA Journal, vol. 39, no. 12, 2001

[8] Markelov G. N., Kudryavtsev A. N., Ivanov M. S. Continuum and kinetic simulation of laminar separated flow at hypersonic speeds. J. of Spacecraft and Rockets, v 37, N 4, 2001

[9] Kogan M. N. Rarefied Gas Dynamics. Plenum, N. Y., 1969

[10] Kashkovsky A. V., Markelov G. N., Ivanov M. S., An object-oriented software design for the direct simulation Monte Carlo method. AIAA Paper 2001-2895, 2001

[11] Jiang G.-S., Shu C.-W. Efficient implementation of weighted ENO schemes. J. Comput. Phys, vol. 126, no. 1

[12] Shakhov E. M. Methods of Rarefied Gas Dynamics. Nauka, Moscow, 1974